



THERMAL BEHAVIOR OF INORGANIC HYDROGEL COMPOSITES

Sinan Temel^[a], Fatma Özge Gökmen^{[a]*} and Elif Yaman^[a]

Keywords: Nano-SiO₂; TiO₂; poly(acrylic acid) (PAA); thermal behavior; hydrogels.

The objective of this work was to examine the effect of inorganic additives on thermal behavior of homo- and hetero-polymeric hydrogel. Nano SiO₂ and TiO₂ doped acrylic acid (AA) based homo-polymeric and acrylic acid/vinyl pyrrolidone (AA/VP) based hetero-polymeric hydrogels were synthesized by using in-situ free radical polymerization technique. Additives were used in the ratio of 0.005, 0.5 and 1 (wt %) on AA based homo-polymeric hydrogels. Hetero-polymeric hydrogels were prepared in ratios of 1:3, 2:2 and 3:1 (AA/VP). Additives were used in only AA/VP (3:1) and they were added 0.5 and 1 (wt %). Thermal behaviour of hydrogels, were investigated by TGA-DTA analysis. The effect of doping on pore structure of hydrogels was demonstrated by SEM analysis. SEM/EDX measurements confirmed the presence of additives in the hydrogels. The dispersions of SiO₂ and TiO₂ on hydrogel were indicated by elemental mapping and their amounts were compared with EDX analysis.

* Corresponding Authors

Fax: +90 228 214 14 27

E-Mail: fatmaozge.gokmen@bilecik.edu.tr

[a] Bilecik Şeyh Edebali University, Central Research Laboratory, Gulumbe Campus, Bilecik, Turkey.

INTRODUCTION

Polymeric materials are chosen of due to the ease of fabrication, flexibility and biocompatible nature as well as their wide range of mechanical, electrical, chemical and thermal behaviors when combined with different materials as composites.¹⁻³ Hydrogels are a class of wet and soft structures, composed by weakly cross-linked polymer matrixes that are hydrophilic three dimensional (3D) network.^{4,5} Hydrogels provide high physical, chemical and mechanical stability in their swollen state.⁶ Hydrogels have been defined which can be modified in order to achieve the unique properties. This special soft-wet structure of hydrogels makes possible them to be applied as biocompatible materials for a variety of biomedical applications including controlled drug delivery systems,⁷ wound dressing,⁸ coating for biosensors,⁹ membranes for bio separation¹⁰ and tissue scaffold engineering.¹¹ Poly(acrylic acid)(PAA) and poly(vinylpyrrolidinone)(PVP) re water soluble synthetic polymers widely used in medical applications. They have low toxicity and are used in medical, food, cosmetics and as a film forming agent.¹²⁻¹⁴ There are many techniques reported for preparation of composites such as sol-gel, in situ dispersion polymerization processing, focused pulsed laser ablation, spin coating, blend process and in situ polymerization, etc.¹⁵⁻¹⁷ Among these, in situ polymerization is a facile approach that involves less time consumption, easy preparation, low cost of production and is also easily scalable. Titanium dioxide (TiO₂) and nano-SiO₂ are considered to best choices of proficient inorganic material due to their outstanding biocompatibility and biomechanical properties (Mohanaprina).

In this study, acrylic acid (AA) and acrylic acid-co-vinyl pyrrolidone (VP) were used as a monomer. Nano SiO₂ and TiO₂ were added to the solution of AA and AA-co-VP (3:1)

with the crosslinking agent and initiator, cross-linked disk-shaped nanocomposite hydrogels were obtained. The nano-SiO₂ and TiO₂ are used as inorganic reinforcement materials and they are supplied by commercially. In the preparation of nanocomposite hydrogels, AA and AA-co-VP monomers were preferred because of their biocompatibility properties. Both homopolymeric and heteropolymeric nanocomposite hydrogels were synthesized by using free radical in-situ polymerization method.

EXPERIMENTAL

Materials used throughout this study; nano-SiO₂ (20-30 nm), TiO₂, acrylic acid, vinyl pyrrolidone, ammonium persulfate, N,N'-methylenebisacrylamide (N,N'-MBAAm) were purchased from Sigma-Aldrich. The cross-linked homo-polymeric and hetero-polymeric hydrogels were prepared by using AA and AA-co-VP monomers in PVC straws. The hydrogel solution containing monomer, initiator, crosslinking agent, solvent, and also nanoparticles was heated in a temperature-controlled water bath (at 80°C) for 2 h. The experimental part was used similar to that described in our previous publication.¹⁸

Measurements

FT-IR analysis were recorded by Perkin Elmer, Spectrum 100 model FT-IR in the range of 400-4000 cm⁻¹. ATR mode was selected and each spectrum was scanned 4 times and worked at a resolution of 4 cm⁻¹. FESEM analyses were performed with Carl Zeiss, Supra 40VP model SEM. Prior to analysis, samples were swollen to equilibrium and then lyophilized. Lyophilized hydrogel discs were sputter coated with Au/Pd alloy. Inorganic particle distributions in nanocomposite hydrogels were determined by applying the mapping technique with the Bruker EDX detector. TGA analyses were performed with the SETARAM simultaneous TG / DTA instrument. The heating was carried out at a temperature range of 30°C-650 °C with a heating rate of 10 °C min⁻¹ in N₂ atmosphere. All analyses were performed with approximately 10 mg of sample in Al₂O₃ pans.

RESULTS AND DISCUSSION

In this study, both synthetic homo-polymeric and two monomers (AA, VP) including hetero-polymeric nanocomposite hydrogels were produced using two separate reinforcing materials (SiO_2 , TiO_2). Thermal behavior, chemical interaction and surface morphology of the obtained hydrogels have been examined and the results are discussed.

Thermal analysis

TGA curves of nano- SiO_2 -free AA hydrogel and AA based homo-polymeric nanocomposite hydrogels with SiO_2 doped in the ratio of 0.05, 0.5 and 1 (wt %) are given in Figure 1. Mass of the 0.5 and 1 wt % SiO_2 doped nanocomposites were found to increase thermal strength. The 0.05 wt % SiO_2 addition had no effect as thermal resistance as compared to that of the pure AA hydrogel. Two-step decomposition curves were obtained at approximately 200-300 °C and 300-400 °C. In both steps 0.5 and 1 wt% SiO_2 was found to increase the heat loss mass resistance.

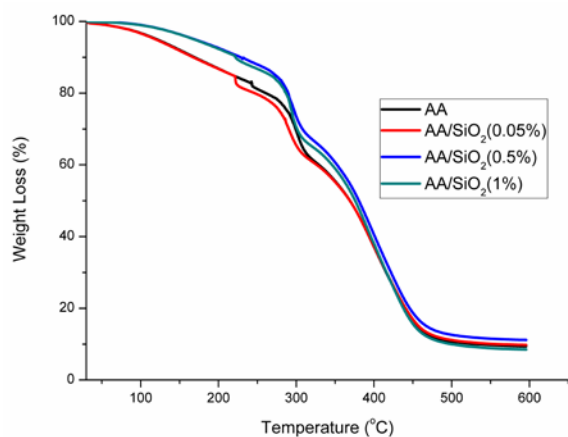


Figure 1. TGA curve of AA hydrogel and 0.05, 0.5, 1 wt % nano- SiO_2 doped AA based nanocomposite hydrogels

Figure 2 shows the TG curves of 0.05, 0.5 and 1 wt % TiO_2 doped AA hydrogels. According to this curve, the contribution of TiO_2 in the ratio of 0.05 wt % increased the thermal degradation resistance of AA based hydrogel.

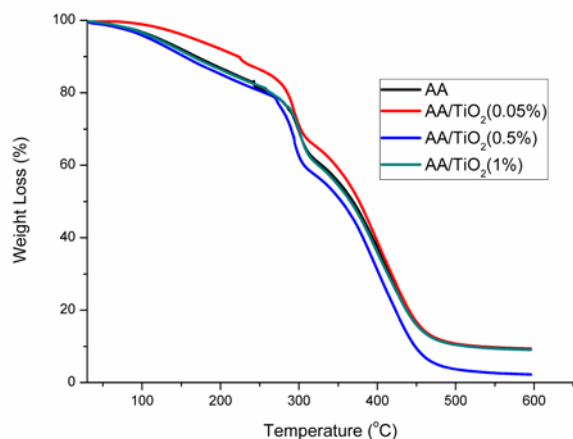


Figure 2. TGA curve of AA hydrogel and 0.05, 0.5, 1 wt% TiO_2 doped AA based composite hydrogels.

As the amount of TiO_2 increased, the thermal resistance of AA hydrogel decreased. The TiO_2 addition did not alter the 2-step chemical degradation process of the pure AA hydrogel.

Figure 3 shows the TGA curve of homo-polymeric AA hydrogel and with optimized AA/VP at a ratio of 1:3, 2:2 and 1:3. The thermal strength of the hetero-polymeric hydrogel obtained with the optimized AA/VP ratios was higher than the homo-polymeric hydrogel. With the increase of VP ratio, not only the thermal strength of the composite was increased, but also the 2-step thermal degradation behavior of acrylic acid was realized in one step. AA and AA/VP obtained in a 3:1 ratio showed similar thermal behavior. For this reason, nano- SiO_2 and TiO_2 additions were compared by applying to both hydrogels.

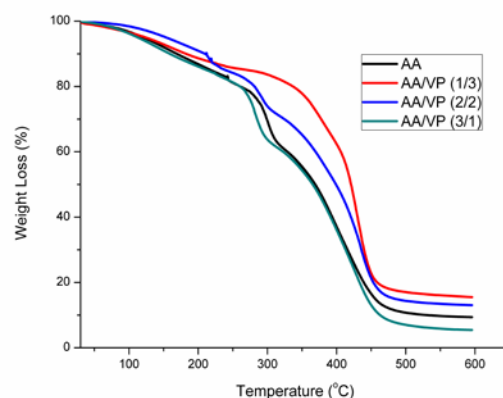


Figure 3. TGA curve of homo-polymeric AA and hetero-polymeric AA/VP in the ratio of 1:3, 2:2 and 3:1 hydrogels.

Figure 4 shows the differential thermal analysis curves of AA/VP (3:1) hetero-polymeric hydrogels with nano- SiO_2 and TiO_2 doping at 0.5 and 1% by mass. Although 0.5 wt % doped SiO_2 did not change the maximum decomposition temperature, it showed the highest thermal resistance behavior compared to other doped and undoped AA/VP (3:1) nanocomposite hydrogels. The maximum thermal decomposition temperature in the second step was most reduced in 1 wt % TiO_2 doped AA/VP (3:1) hydrogel.

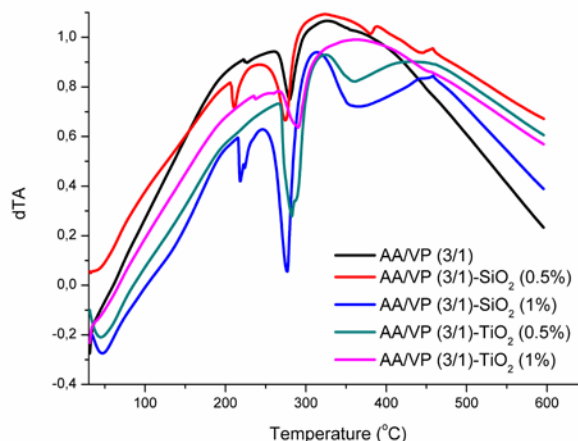


Figure 4. Differential thermal analysis of nano- SiO_2 and TiO_2 (0.5 and 1 wt %) doped and undoped hetero-polymeric AA/VP (3:1) hydrogels.

Table 1. Thermogravimetric data of the SiO₂ and TiO₂ additive AA-homopolymeric and AA/VP-heteropolymeric nanocomposite hydrogels.

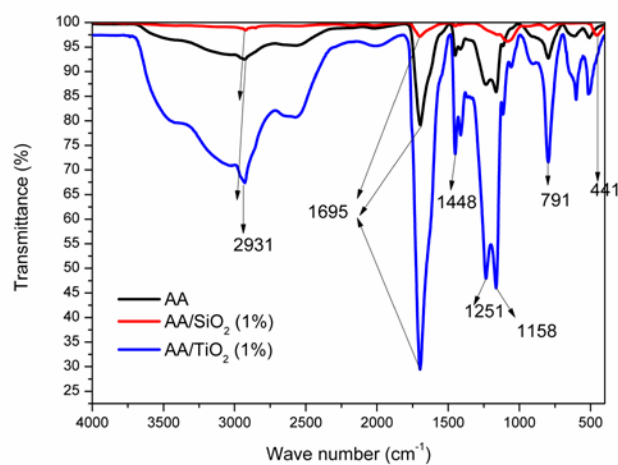
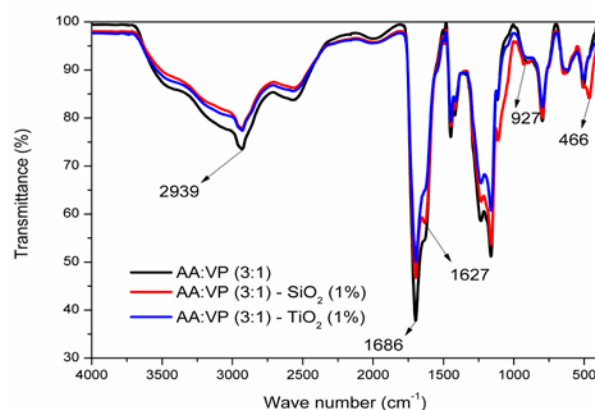
AA, %	VP, %	SiO ₂ , wt. %	TiO ₂ , wt. %	degradation step, °C		T _{d(max)} , °C	Weight loss (%) at degradation steps, °C	
				1 st	2 nd		1 st	2 nd
100	0	-	-	30-249	249-343	245;	18	25
100	0	0.005	-	30-225	225-345	225;	16	27
100	0	0.5	-	30-275	275-342	228;	15	22
100	0	1	-	30-227	227-307	222;	11	23
100	0	-	0.05	30-240	240-297	227;	12	15
100	0	-	0.5	30-268	268-342	275	20	27
100	0	-	1	30-252	252-345	297	8	25
25	75	-	-	30-293	293-497	384;	16	67
50	50	-	-	30-222	222-308	220;	12	15
75	25	-	-	30-265	265-340	280	21	15
75	25	0.5	-	30-215	215-290	212;	13	22
75	25	1	-	30-252	252-315	215;	16	22
75	25	-	0.5	30-268	268-487	282;	18	18
75	25	-	1	30-273	273-336	292	20	21

In Table 1, the thermal decomposition steps of AA homopolymeric hydrogel with nano-SiO₂ and TiO₂ added in mass ratios of 0.005, 0.5, 1%; AA/VP hetero-polymeric hydrogels which were prepared in different ratios (1:3, 2:2, 3:1) as well as AA/VP (3:1) hydrogel with nano-SiO₂ and TiO₂ added at a ratio of 0.5 and 1 wt%, the maximum decomposition temperatures in these steps of all samples and the percent mass losses in the thermal decomposition intervals are given. According to this table, water separation in the hydrogel structure and thermal decomposition of the hydrogel structures occurred in the first step (30-250 °C). Chemical degradation in AA and AA/VP based hydrogels occurred in 2-steps due to thermal behavior of acrylic acid.¹⁹ Thermal degradation in the second step occurred between about 250-350 °C. As a result of the addition to homopolymeric hydrogels, the maximum thermal decomposition was observed in the AA-TiO₂ composite hydrogel with 0.5 and 1 wt % TiO₂. There was a low increase in the 1 % TiO₂ addition at the maximum thermal decomposition temperature in the second step. Other additions did not cause a change in the maximum decomposition temperature. AA:VP hetero-polymers were prepared using AA and VP monomers in a 1:3, 2:2 and 3:1 ratio. Accordingly, as the VP amount increased, the thermal behavior changed and the maximum decomposition temperature increased by approximately 100 °C (at 384 °C).

FTIR analysis

In Figure 5, the FTIR spectrum of 1 wt % nano-SiO₂ and TiO₂ doped and undoped AA hydrogels are given. Since the chemical effect of the additives on the hydrogel were not observed in the amounts of 0.05 and 0.5 wt %, the comparison was made in 1 wt % SiO₂ and TiO₂ doping results. OH groups of the nanocomposite hydrogels gave a broad peak at approximately 2700-3600 cm⁻¹. The band at 1695 cm⁻¹ is the C = O tensile vibration of the COOH group of AA. The symmetrical stress peak of Si-O-Si was observed in 1050 cm⁻¹ and 441 cm⁻¹ on 1 wt % SiO₂ added AA hydrogel.

The chemical interaction of Ti-O with hydrogel was not found in the spectrum because of large particle size agglomeration.

**Figure 5.** FTIR spectrum of 1 (wt %) nano-SiO₂ and TiO₂ doped and undoped AA hydrogel.**Figure 6.** FTIR spectrum of 1 (wt %) nano-SiO₂ and TiO₂ doped and undoped AA/VP (3:1) hydrogels.

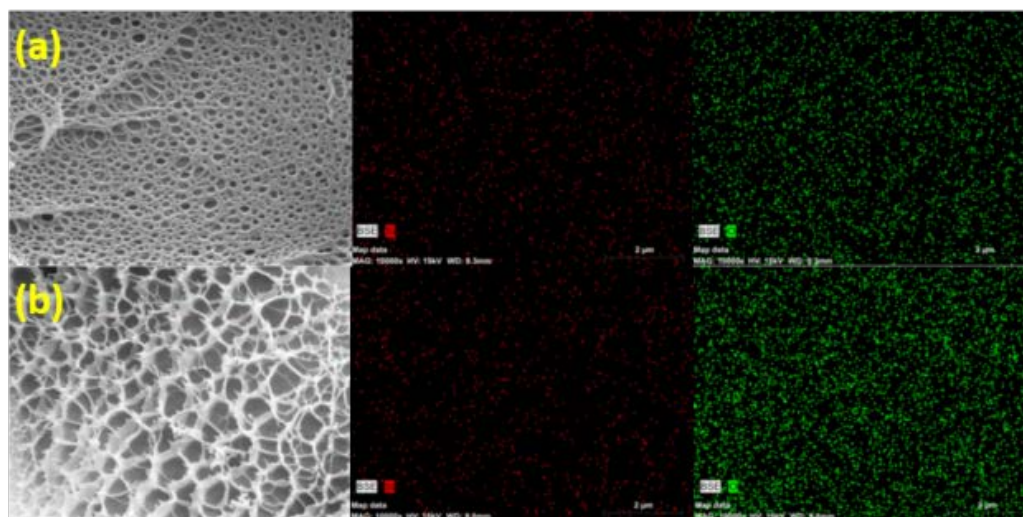


Figure 7. SEM images and elemental map distribution of (a) SiO₂ (wt %) doped AA hydrogel (b) SiO₂ (wt%) doped AA/VP (3:1) hydrogel.

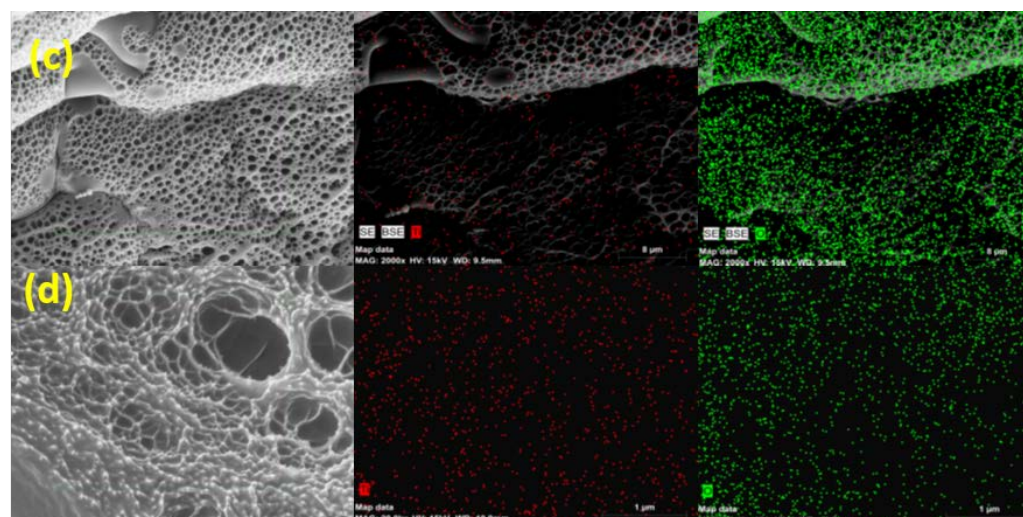


Figure 8. SEM images and elemental map distribution of (c) TiO₂ (wt %) doped AA hydrogel (d) TiO₂ (wt %) doped AA/VP (3:1) hydrogel.

The FTIR spectra of a 1 wt % nano-SiO₂ and TiO₂ doped and an undoped AA/VP (3:1) hetero-polymeric hydrogel's are given in Figure 6. According to spectrum, Si-O-Si stress interaction of SiO₂ doped at 466 cm⁻¹ was observed. No structural change was observed in TiO₂ doped AA/VP (3:1) composite hydrogel.

SEM analysis

SEM images of SiO₂ doped AA (Fig. 7 (a)) and AA/VP (3:1) (Fig. 7 (b)) hydrogels, also silica (Si) and oxygen (O) distribution are given in Fig 7. Homogeneous pore structures were observed in both hydrogels. Si and O distributions are homogeneous on the hydrogels surface. SEM images of TiO₂ doped AA (Fig. 8 (c)) and AA/VP (3:1) (Fig. 8 (d)) hydrogel, and titanium (Ti), oxygen (O) distribution are shown in Fig 8. The pore distributions of TiO₂ doped hydrogels are not homogeneous. In the structure, the Ti and

O distributions were distributed homogeneously on the polymer matrix. The EDX analysis results of all obtained samples are given in Table 2 in percent by atom. EDX signals are seen low, especially in nano-SiO₂ additive, since there is low percentage mass addition. The presence of SiO₂ on the hydrogel can be demonstrated by an increase in the total oxygen content.

CONCLUSION

It was observed that low amount (0.05 wt. %) of SiO₂ had no thermal contribution to homo-polymeric AA hydrogel. 0.5 and 1 wt% nano-SiO₂ increased the thermal degradation resistance of AA hydrogel. The TiO₂ additive, which was not used in the nanoscale, decreased the thermal strength of the AA-TiO₂ composite hydrogel, as expected, due to agglomeration as the amount of doping increased.

Table 2. Atomic % of C, O, N, Si and Ti contents in homo- and hetero-polymeric nanocomposite hydrogels.

Samples	C	O	N	Si	Ti
AA	59.11	40.89	-	-	-
AA-SiO ₂ (0.05%)	57.43	42.57	-	0.00	-
AA-SiO ₂ (0.5%)	57.90	42.09	-	0.00	-
AA-SiO ₂ (1%)	57.63	42.34	-	0.03	-
AA-TiO ₂ (0.05%)	56.74	43.23	-	-	0.03
AA-TiO ₂ (0.5%)	57.52	42.47	-	-	0.01
AA-TiO ₂ (1%)	60.72	39.21	-	-	0.07
AA:VP (1:3)	63.84	27.74	8.42	-	-
AA:VP (2:2)	60.55	33.63	5.82	-	-
AA:VP (3:1)	58.12	38.88	3.00	-	-
AA/VP (3:1)- SiO ₂ (0.5%)	59.18	37.65	3.17	0.00	-
AA/VP (3:1)- SiO ₂ (1%)	57.96	38.23	3.81	0.00	-
AA/VP (3:1)- TiO ₂ (0.5%)	62.58	33.36	2.96	-	1.41
AA/VP (3:1)- TiO ₂ (1%)	71.26	27.59	1.12	-	0.02

The best thermal degradation resistance was seen in AA hydrogel with 0.05 TiO₂ doped. The AA/VP hetero-polymeric hydrogel was optimized by preparing in 1:3, 2:2 and 3:1 AA:VP ratios and 3:1 AA/VP hydrogel was selected as the hydrogel. When the amount of VP increased from two different monomers, apart from the increase in thermal strength, degradation began to occur in one step. Due to the effect of reinforcing materials on hydrogels, AA and AA/VP (3:1) hydrogels with similar thermal behaviors were used as matrix in the composite.

Changing of the chemical structure of TiO₂ and SiO₂ doped homo-polymeric and hetero-polymeric hydrogels was investigated by FTIR analysis. Binding vibrations of SiO₂, homogeneously distributed on AA in nanoscale, were obtained in the FTIR spectrum. Due to the larger particle size, no structural change was observed in the same amount of TiO₂ doped AA/VP (3:1) composite hydrogel. In homo-polymeric and hetero-polymeric hydrogels, the pore and Si, O element distribution is homogeneous as a result of nano-SiO₂ doping. As a result of TiO₂ doping with large particle size, both polymer matrices lost homogeneity in pore distribution.

ACKNOWLEDGMENT

The authors thank to the Bilecik Seyh Edebali University Central Research Laboratory for the characterization measurements. Also, would like to thank Hacettepe University, Hünitek Center for TG-DTA analysis.

REFERENCES

- Mohanapriya, S., Mumjitha, M., Purna-Sai, K., Raj, V., Fabrication and Characterization of Poly(vinyl alcohol)-TiO₂ Nanocomposite films for Orthopaedic applications *J. Mech. Behav. Biomed.*, **2016**, *63*, 141-156. <http://dx.doi.org/10.1016/j.jmbbm.2016.06.009>
- Tanan, W., Panichpakdee, J., Saengsuwan, S., Novel Biodegradable Hydrogel Based on Natural Polymers: Synthesis, Characterization, Swelling/Reswelling and Biodegradability, *Eur. Polym. J.*, **2019**, *112*, 678-687. <https://doi.org/10.1016/j.eurpolymj.2018.10.033>
- Balasubramanian, R., Kim, S. S., Lee, J., Lee, J., Effect of TiO₂ on highly elastic, stretchable UV protective nanocomposite films formed by using a combination of k-Carrageenan, xanthan gum and gellan gum, *Int. J. Biol. Macromol.*, **2019**, *123*, 1020-1027. <https://doi.org/10.1016/j.jbiomac.2018.11.151>
- Abdollahi, R., Taghizadeh, M. T., Savani, S., Thermal and mechanical properties of graphene oxide nanocomposite hydrogel based on poly (acrylic acid) grafted onto amylose, *Polym. Degrad. Stabil.*, **2018**, *147*, 151-158. <https://doi.org/10.1016/j.polymdegradstab.2017.11.022>
- Rasool, A., Ata, S., Islam, A., Stimuli responsive biopolymer (chitosan) based blend hydrogels for wound healing application, *Carbohydr. Polym.*, **2019**, *203*, 423-429. <https://doi.org/10.1016/j.carbpol.2018.09.083>
- Raphael, M., Springer Science Business Media, LLC., Springer-Verlag, New York, Kinam Park Teruo Okano, **2010**. <https://www.springer.com/gp/book/9781441959188>
- Sagiri, S. S., Singh, V. K., Kulanthaivel, S., Banerjee, I., Basak, P., Battachrya, M. K., Pal, K., Stearate organogel-gelatin hydrogel based bigels: Physicochemical, thermal, mechanical characterizations and in vitro drug delivery applications, *J. Mech. Behav. Biomed. Mater.*, **2015**, *43*, 1-17. <https://doi.org/10.1016/j.jmbbm.2014.11.026>
- Li, D., Ye, Y., Li, D., Li, X., Biological properties of dialdehyde carboxymethyl cellulose crosslinked gelatin-PEG composite hydrogel fibers for wound dressings, *Carbohydr. Polym.*, **2016**, *137*, 508-514. <https://doi.org/10.1016/j.carbpol.2015.11.024>
- Wang, Y., Papadimitrakopoulos, F., Burgess, D. J., Polymeric "smart" coatings to prevent foreign body response to implantable biosensors, *J. Control. Release*, **2013**, *169(3)*, 341-347. <https://doi.org/10.1016/j.jconrel.2012.12.028>
- Huang, R., Kostanski, L. K., Filipe, C. D. M., Ghosh, R., Environment-responsive hydrogel-based ultrafiltration membranes for protein bioseparation, *J. Membr. Sci.*, **2009**, *336(1-2)*, 42-49. <https://doi.org/10.1016/j.memsci.2009.03.002>
- Fan, C., Wang, D. A., A biodegradable PEG-based micro-cavitary hydrogel as scaffold for cartilage tissue engineering, *Eur. Polym. J.*, **2015**, *72*, 651-660. <https://doi.org/10.1016/j.eurpolymj.2015.02.038>
- Krezovic, B. D., Miljkovic, M. G., Stojanovic, S. T., Najman, S. J., Filipovic, J. M., Tomic, S. Lj., Structural, thermal, mechanical, swelling, drug release, antibacterial and cytotoxic properties of P(HEA/IA)/PVP semi-IPN hydrogels, *Chem. Eng. Res. Des.*, **2017**, *121*, 368-380. <http://dx.doi.org/10.1016/j.cherd.2017.03.030>
- Wang, Y., Cao, Z., Wu, J., Ma, C., Qiu, C., Zhao, Y., Shao, F., Wang, H., Zheng, J., Huang, G., Mechanically robust, ultrastretchable and thermal conducting composite hydrogel and its biomedical applications, *Chem. Eng. J.*, **2019**, *360*, 231-242. <https://doi.org/10.1016/j.cej.2018.11.223>
- Chen, K., Liu, J., Yang, X., Zhang, D., Preparation, optimization and property of PVA-HA/PAA composite hydrogel, *Mat. Sci. Eng. C-Mater. Biol. Appl.*, **2017**, *78*, 520-529. <http://dx.doi.org/10.1016/j.msec.2017.04.117>
- Hussain, F., Hojjati, M., Okamoto, M., Gorga, R. E., Review article: Polymer-matrix Nanocomposites, Processing, Manufacturing, and Application: An Overview, *J. Compos. Mater.*, **2006**, *40*, 1511-1575. <https://doi.org/10.1177/0021998306067321>
- Niu, H., Li, X., Li, H., Fan, Z., Ma, J., Guan, J., Thermosensitive, fast gelling, photoluminescent, highly flexible, and

- degradable hydrogels for stem cell delivery, *Acta Biomater.*, **2019**, 83, 96-108.
<https://doi.org/10.1016/j.actbio.2018.10.038>
- ¹⁸Mittal, H., Ray, S. S., A study on the adsorption of methylene blue onto gum ghatti/TiO₂ nanoparticles-based hydrogel nanocomposite, *Int. J. Biol. Macromol.*, **2016**, 88, 66-80.
<http://dx.doi.org/10.1016/j.ijbiomac.2016.03.032>
- ¹⁹Gökmen, F. Ö., Pekel, B. N., Synthesis and Characterization of N-[3-(Dimethylamino)propyl]methacrylamide/(nano SiO₂, amine-modified nano SiO₂, and expanded perlite) Nanocomposite Hydrogels, *Eur. Chem. Bull.*, **2017**, 6(11), 514-418. DOI: 10.17628/ecb.2017.6. 514-518.
- ²⁰Kabra, S., Katara, S., Rani, A., Characterization and study of Turkish perlite, *Int. J. Innov. Res. Sci. Eng. Tech.*, **2013**, 2, 4319-4326.

Received: 24.10.2019.

Accepted: 16.11.2019